Science of the Total Environment 496 (2014) 678–687

Contents lists available at ScienceDirect

Science of the Total Environment

journal homepage: www.elsevier.com/locate/scitotenv

Gaseous mercury fluxes from forest soils in response to forest harvesting intensity: A field manipulation experiment

M. Mazur [a], C.P.J. Mitchell [a,*], C.S. Eckley [b,1], S.L. Eggert [c], R.K. Kolka [c], S.D. Sebestyen [c], E.B. Swain [d]

[a] University of Toronto Scarborough, Department of Physical and Environmental Sciences, 1265 Military Trail, Toronto, ON M1C 1A4, Canada
[b] Meteorological Service of Canada, Environment Canada, 4905 Dufferin Street, Toronto, ON M3H 5T4, Canada
[c] Northern Research Station, USDA Forest Service, 1831 Hwy 169 E, Grand Rapids, MN 55744, United States
[d] Minnesota Pollution Control Agency, St. Paul, MN 55155, United States

HIGHLIGHTS

- We investigated forestry impacts on gaseous Hg flux in a field experiment.
- We measured ambient Hg fluxes and fluxes from added enriched Hg isotope tracers.
- Biomass harvesting following clearcut had the greatest impact on ambient fluxes.
- These impacts were seasonally restricted to the leaf-out growing season.
- Isotope results suggest emissions dominated by legacy Hg pools.

GRAPHICAL ABSTRACT

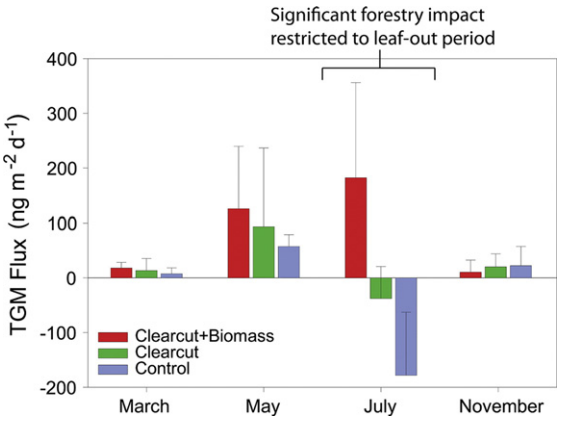

ARTICLE INFO

Article history:
Received 29 January 2014
Received in revised form 13 June 2014
Accepted 13 June 2014
Available online 30 June 2014

Keywords:
Forest
Gaseous mercury emissions
Clearcut
Biomass harvesting
Mercury isotope
Solar radiation

ABSTRACT

Forest harvesting leads to changes in soil moisture, temperature and incident solar radiation, all strong environmental drivers of soil–air mercury (Hg) fluxes. Whether different forest harvesting practices significantly alter Hg fluxes from forest soils is unknown. We conducted a field-scale experiment in a northern Minnesota deciduous forest wherein gaseous Hg emissions from the forest floor were monitored after two forest harvesting prescriptions, a traditional clear-cut and a clearcut followed by biomass harvest, and compared to an un-harvested reference plot. Gaseous Hg emissions were measured in quadruplicate at four different times between March and November 2012 using Teflon dynamic flux chambers. We also applied enriched Hg isotope tracers and separately monitored their emission in triplicate at the same times as ambient measurements. Clearcut followed by biomass harvesting increased ambient Hg emissions the most. While significant intra-site spatial variability was observed, Hg emissions from the biomass harvested plot (180 ± 170 ng m^{-2} d^{-1}) were significantly greater than both the traditional clearcut plot (-40 ± 60 ng m^{-2} d^{-1}) and the un-harvested reference plot (-180 ± 115 ng m^{-2} d^{-1}) during July. This difference was likely a result of enhanced Hg^{2+} photoreduction due to canopy removal and less shading from downed woody debris in the biomass harvested plot. Gaseous Hg emissions from more recently deposited Hg, as presumably representative of isotope tracer measurements, were not significantly influenced by harvesting. Most of the Hg tracer applied to the forest floor became sequestered within the ground vegetation and debris, leaf litter, and soil. We observed a dramatic lessening of tracer Hg

* Corresponding author. Tel.: +1 416 208 2744.
E-mail address: carl.mitchell@utoronto.ca (C.P.J. Mitchell).
[1] Now at: U.S. Enviornmental Protection Agency, Region 10, 1200 Sixth Avenue, Seattle, WA, 98101, United States.

http://dx.doi.org/10.1016/j.scitotenv.2014.06.058

emissions to near detection levels within 6 months. As post-clearcutting residues are increasingly used as a fuel or fiber resource, our observations suggest that gaseous Hg emissions from forest soils will increase, although it is not yet clear for how long such an effect will persist.

1. Introduction

Gaseous mercury (Hg) is a problematic pollutant because its relatively long atmospheric lifetime allows for long-range transport and deposition in remote locations, where it has the potential to be methylated and subsequently accumulated in biota (Schroeder and Munthe, 1998). Mercury in soil, whether present due to geologic enrichment or atmospheric deposition, can be reduced to volatile elemental mercury (Hg^0) and emitted to the atmosphere through a number of complex processes (Lin et al., 2010). Soil Hg concentrations and mineralogy control the quantity of Hg available for emission (Miller et al., 2011). Soil emissions have been shown to vary temporally in response to numerous environmental variables, including soil moisture (Gustin and Stamenkovic, 2005; Song and Van Heyst, 2005; Xin et al., 2007), air temperature (Kim et al., 2012; Lin et al., 2010), soil temperature (Johnson et al., 2003; Magarelli and Fostier, 2005; Moore and Castro, 2012; Sigler and Lee, 2006; Zhang et al., 2001), atmospheric Hg concentrations (Kuiken et al., 2008b; Wallschlager et al., 2002), and incident solar radiation (Carpi and Lindberg, 1998; Converse et al., 2010; Gustin et al., 2002; Moore and Carpi, 2005; Poissant and Casimir, 1998; Stamenkovic and Gustin, 2007; Xin et al., 2006). Typically, several of these variables act synergistically in their impact on Hg emission.

Several studies have found that incident solar radiation is the single strongest control on gaseous Hg emissions (Ericksen et al., 2005; Gustin et al., 2002; Kuiken et al., 2008a). Where solar radiation is able to penetrate soil it facilitates photo-reduction of soil bound Hg^{2+} to gaseous Hg^0, which is then emitted to the atmosphere from the soil surface (Carpi and Lindberg, 1997; Gustin et al., 2002; Moore and Carpi, 2005). Hg fluxes tend to be highest during periods of peak solar inputs. However even during moderate levels of solar radiation (as little as 70 W m^{-2}), Hg emission from soil can continue (Gustin et al., 2006; Kuiken et al., 2008a). As solar radiation heats soils and air, strong associations have also been identified among soil temperature, air temperature, and gaseous Hg emissions (Kim et al., 2012; Lin et al., 2010; Margarelli and Fostier, 2005; Moore and Castro, 2012; Zhang et al., 2001) because these factors effectively lower the activation energy for Hg reduction (18.0–24.9 kcal mol^{-1} — Carpi and Lindberg, 1998). Increasing soil moisture may further enhance (through upward transport of Hg via capillary action) or suppress (saturated soils reduce photo-reduction efficacy) Hg emissions depending on the degree of wetting (Gustin and Stamenkovic, 2005; Johnson et al., 2003; Lin et al., 2010; Song and Van Heyst, 2005).

Mercury emissions from forest soils vary seasonally in response to changes in canopy cover, which affects solar radiation, temperature, and soil moisture (Choi and Holsen, 2008; Kuiken et al., 2008a). Estimates of the solar radiation that penetrates mature deciduous canopies are between 20 and 58%, thus Hg fluxes from forest soils are typically lower in the growing season than in leaf-free seasons (Denkenberger et al., 2012; Gustin et al., 2004; Gustin and Stamenkovic, 2005; Kuiken et al., 2008a; Schroeder et al., 2005; Sigler and Lee, 2006). Higher magnitude Hg emissions in the spring and autumn typically occur due to the lack of foliage and therefore higher proportion of incident radiation able to penetrate to the forest floor (Choi and Holsen, 2008; Kuiken et al., 2008a, 2008b). Fluxes from soils in most northern deciduous forests are considered negligible in the winter due to persistent snow cover throughout most of the season (Denkenberger et al., 2012). Currently there are few published observations of Hg fluxes from forests through seasons (Choi and Holsen, 2008; Kuiken et al., 2008a). As such the regulation of Hg fluxes by forest vegetation is relatively poorly documented (Schroeder et al., 2005).

North American deciduous forests are an important source of timber for pulp and paper production and disturbance of forest vegetation via harvesting is common in many regions. Clearcutting involves the complete removal of stems suitable for the production of wood-based products from a forested area, resulting in a large open area. Woody debris (material not economically suitable for the production of wood based products, including branches, underbrush, and small trees) is typically left on-site. Recently however, with increased incentive for sustainable harvesting and the development of new uses for woody biomass (e.g. for renewable fuels as has been legislated in the 2007 U.S. Energy Independence and Security Act or as a fiber resource), removal of woody debris after harvesting has increased (Janowiak and Webster, 2010). Though such techniques make more efficient use of woody biomass, the removal of more woody material from clearcut sites may ultimately increase the intensity of disturbance to these sites, removing shading and potentially increasing Hg emissions. Studies examining the direct impacts of forestry operations on soil Hg fluxes are very limited (Magarelli and Fostier, 2005). Currently, the only work performed on this topic has been from tropical rainforests in South America where Hg emissions have been shown to increase in response to deforestation (Almeida et al., 2009; Magarelli and Fostier, 2005). However these results may not be directly transferable to the forestry sector in higher latitude climates.

Enriched stable Hg isotope tracers (herein Hg tracers) are useful in the determination of Hg fate within environmental systems (Hintelmann and Evans, 1997). Several studies have utilized Hg tracers to examine the fate of contemporary deposition on soil surfaces (Ericksen et al., 2005; Xin et al., 2007); however, few measurements of emitted Hg tracers have been made in forested environments and none have looked at the impacts of forest harvesting (Hintelmann et al., 2002; Munthe et al., 2001). These studies have shown that added Hg tracers (presumably representing recently deposited Hg) quickly become sequestered into the soil (Ericksen et al., 2005; Hintelmann et al., 2002; Munthe et al, 2001). Once the Hg has infiltrated into the soil column with rainwater, its ability to be emitted is greatly reduced due to the lack of solar radiation, which only penetrates a very shallow depth below the soil surface (Xin et al., 2007; Carpi and Lindberg, 1997). Of the Hg tracer emitted back to the atmosphere, some (0.1 to 3%) is emitted within 24 h of deposition (Ericksen et al., 2005; Xin et al., 2007). Emissions quickly decline in weeks to months following deposition, to barely detectable levels and on an annual basis account for only ~6–8% of the original amount deposited (Ericksen et al., 2005; Hintelmann et al., 2002). Studies that have scaled surface Hg emissions annually have shown that forests (and other natural background surfaces) are a large net sink for atmospheric Hg, with inputs from wet and dry deposition exceeding levels of Hg emissions (Hartman et al, 2009; Kuiken et al., 2008a; Denkenberger et al., 2012). Given the net accumulation of Hg in forest ecosystems, it is critical to understand the potential impact of clearcutting and biomass harvesting on surface–air Hg flux dynamics.

This study aims to determine the effects of two common forms of forest harvesting, clearcutting and clearcutting with additional biomass (woody debris) removal, on Hg fluxes from forest soils. This study also expands our current understanding of seasonal Hg emission variability and the fate of contemporary Hg deposition to soils in northern forested environments. We analyzed ambient gaseous Hg emissions across seasons to elucidate some of the processes controlling observed Hg emissions. Additionally we used a field-scale enriched stable Hg isotope tracer application to represent the fate of newly deposited Hg in forest soils. We expected that both ambient and tracer Hg emissions would

increase proportionally with the intensity of forest harvest, due to a combination of the removal of vegetative shading, which increases solar radiation input and reduces evapotranspirative losses from forest soils, leading to increased soil moisture.

2. Methods

2.1. Experimental design

2.1.1. Site description and experimental approach

This experiment was conducted on a north-facing upland soil hillslope in the S7 watershed of the Marcell Experimental Forest in north-central Minnesota, USA (47° 31′ 21″ N, 93° 28′ 7″ W; Fig. 1). The climate is strongly continental with mean annual precipitation of 780 mm and a mean annual air temperature of 3.4 °C, ranging from an average of 19 °C in July to −15 °C in January (Sebestyen et al., 2011). The mean slope of the hillslope is 10° and drains into a peatland at its foot. The upland mineral soils were formed by the Wisconsinan glacial drift. Surface soils are sandy loams, overlain by a thin, organic-rich O horizon and underlain by low permeability glacial till. Overstory vegetation mainly consisted of mature quaking aspen (*Populus tremuloides*), sugar maple (*Acer saccharum*), paper birch (*Betula papyrifera*), and balsam poplar (*Populus balsamifera*) with lower abundances of basswood (*Tilia Americana*), ironwood (*Carpinus caroliniana*) and mountain maple (*Acer spicatum*; Sebestyen et al., 2011). Understory vegetation consisted primarily of seedlings with intermixed big-leaved aster (*Eurybia macrophylla*), bracken fern (*Pteridium aquilinum*), largeflower bellwort (*Uvularia grandiflora*), blue bead lily (*Clintonia borealis*) and various mosses. The forest floor retains a litter layer well into the growing season; however utilization by non-native invasive earthworms generally reduces the quantity of leaf litter significantly towards the end of the growing season.

Three adjacent plots of approximately equal size (~0.3 ha) and of equivalent slope and soil composition were delineated adjacent to one another on the hillslope. In March 2012, while the ground was still snow covered, the forest was harvested on two of the three plots. Trees with a diameter at breast height (DBH) greater than 2.5 cm were felled on each of these plots similar as would occur in a normal forestry operation for pulp and paper. However, the handling of woody debris after clearcut differed between the two harvested plots. One plot was left with woody debris <2.5 cm in diameter in place after the removal of merchantable timber (henceforth referred to as the clearcut plot; Fig. 1). The other clearcut plot was cleared of ~85% of woody debris to simulate a biomass removal operation (this plot is henceforth referred to as the clearcut + biomass plot; Fig. 1). The third plot was left as an unharvested control (referred to as the control plot; Fig. 1). Two different Hg tracers, each with a unique enriched stable isotope, were applied to the study site in May 2011 and May 2012, to help elucidate whether current deposition, as presumably representative of the added Hg tracers (Harris et al., 2007), behaved differently from the legacy Hg pool. The Hg tracer applied in May 2011 contained 94.3% enriched ^{200}Hg while in May 2012 the Hg tracer was 42.1% enriched ^{204}Hg. Our preparation of isotope solutions closely followed previous protocols used in the METAALICUS experiment (Hintelmann et al., 2002; Harris et al., 2007). Our stock isotope solutions were in the form $HgCl_2$. Application solutions were mixed in backpack mounted sprayers using enough of the $HgCl_2$ stock solution in 18 l of pH adjusted (pH = 5.4) tap water in each backpack sprayer such that when sprayed evenly onto a 650 m^2 area, the resulting

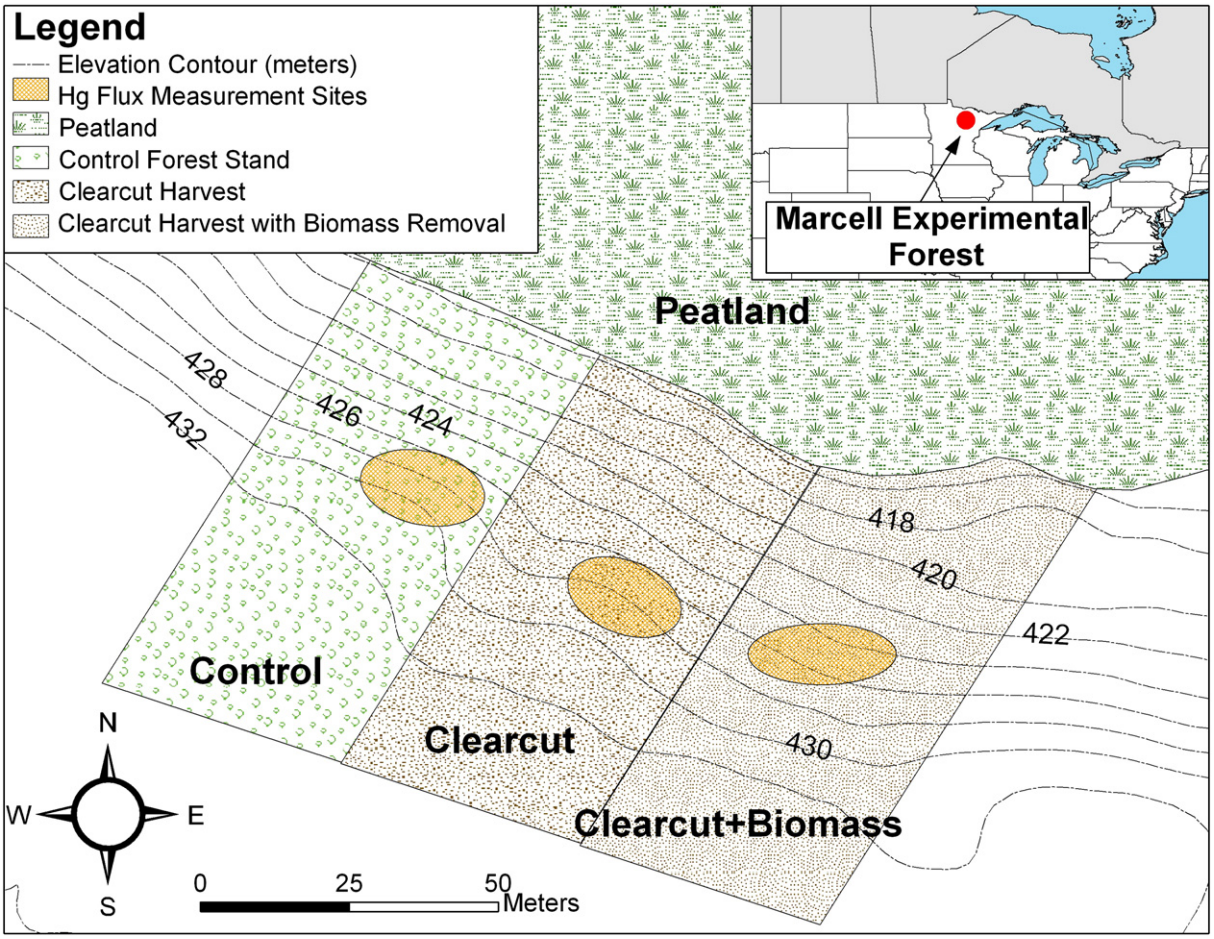

Fig. 1. Map of the study site. Harvesting treatments and plot names are labeled. Locations of mid-slope measurement sites are indicated on each plot. See text for details.

deposition would equal 14 μg m^{-2}. Three researchers wearing the sprayers added the isotope solutions simultaneously under low sunlight and lightly raining conditions, until a total of 14 sprayers full of isotope solution were added to the entire hillslope.

2.1.2. Measurement and sampling details

Gaseous Hg fluxes were measured during the months of March (post-snowmelt/early spring), May (spring), July (summer/peak growing season), and November (autumn following senescence) in 2012. A small subset of measurements for tracer Hg emissions was also made during the growing season prior to the forest harvesting operations (August, 2011). We measured ambient total gaseous Hg (TGM) fluxes in quadruplicate (two at a time for 24-hour periods each) on each of the three plots using Teflon dynamic flux chambers (0.036-m^2 footprint, 6.5-cm height and 2.0-l volume as per Eckley et al., 2010) connected to a gaseous Hg analyzer (Tekran 2537A Gaseous Mercury Analyzer). We measured tracer Hg gaseous fluxes in triplicate over the same 2-day period, also using Teflon dynamic flux chambers, but with gold traps connected to calibrated air pumps. Tracer fluxes were completed over a period of one to 3 h at solar noon, to measure peak fluxes, and at night, to approximate baseline fluxes. For any one season, measurements were therefore completed over a period of six days to cover all three experimental treatments. Sampling was conducted at mid-slope locations to minimize plot edge effects (e.g., shading from control plot) and sites were randomly chosen throughout the study. Sampling locations were not re-used because soil and leaf litter samples were collected directly beneath chambers immediately after Hg emission measurements. Leaf litter samples consisted of all free leaf litter and organic debris within the footprint of the dynamic flux chamber. Soil samples consisted of the top 2 cm soil from beneath the flux chamber. Leaf litter and soil samples were kept frozen until analysis. Before sampling, the flux chambers were soaked in 10% HNO_3 and rinsed thoroughly with deionized water (18.2 MΩ cm). Blank measurements to verify the cleanliness of the flux chambers were made in the field with the dynamic flux chambers placed over clean polycarbonate film above the soil surface the day before the commencement of gaseous Hg emission measurements.

For TGM emission measurements, the sampling flow rate of the Tekran 2537A sampler was 1.5 l min^{-1}. The instrument was calibrated every 24 h during sampling using the instrument's internal mercury permeation source. Injections from an external calibration unit (Tekran 2505) were used to verify accuracy of the internal permeation source. A four-port sampling manifold (Tekran 1115 Synchronized Multi-Port Sampling System) was plumbed to the Tekran 2537A for switching air accumulation among 4 points (an inlet and outlet port on each of two dynamic flux chambers) to allow near simultaneous duplication of measurements (Carpi and Lindberg, 1997). Each flux measurement consisted of two consecutive measurements of each inlet/outlet (one measurement from each gold cartridge in the Tekran 2537A) allowing an overall sampling frequency of one flux measurement every 20 min. A secondary bypass pump was utilized to draw air through the non-analyzed lines at a rate of 1.5 l min^{-1} to match the sampling rate of the Tekran 2537A.

Air samples for measuring gaseous tracer Hg fluxes were collected using air sampling pumps (Buck Libra Plus LP-5) drawing air through gold traps at a rate of 1.5 l min^{-1}. Two gold traps were used to simultaneously collect gaseous Hg samples adjacent to one of the inlet ports and from the outlet port of a dynamic flux chamber (Carpi and Lindberg, 1997). Gold traps consisted of quartz tubes with gold-coated silica media for the adsorption of Hg (Graydon et al., 2006). A bubble flow calibrator (mini-Buck Calibrator M-5) was used to verify the flow rate of air through the gold traps at the beginning and end of every measurement. Gold traps were blanked and sealed before transport to the field and remained sealed except when used for sampling.

Energy and soil moisture variables were continuously measured at 1-min intervals in close proximity (<5 m) to the flux chambers throughout each sampling campaign. These variables included air temperature (Campbell Scientific CR1000 internal temperature sensor), soil temperature at 2 cm depth (BetaTherm 100K6A1B thermistor), volumetric soil moisture content across the top 5 cm of the soil column (CS650 Soil Water Content Reflectometer), and incident solar radiation at the soil surface (Kipp & Zonen SPLITE2 Silicon Pyranometer). Additionally throughout 2012, volumetric soil moisture at 1 cm (EC-5 Soil Moisture Smart Sensor), and incoming solar radiation at 0.25 m above the ground (Silicon Pyranometer) were continuously measured at 15-minute intervals at a mid-slope location in each plot. For comparison to open-canopy energy, pyranometer data were also obtained from an open peatland site, Bog Lake, located 2.4 km south of our hillslope plots (Sebestyen et al., 2011).

The quantity of downed woody debris was inventoried before and after the treatments using the line intersect method described by Brown (1974). Woody debris was categorized into two size classes, coarse woody debris (CWD) and fine woody debris (FWD), corresponding to diameters greater than and less than 7.6 cm (US Forest Service, 2010). Volume per unit area was calculated separately for size classes and summed using the methods of van Wagner (1968, 1982), van Wagner and Wilson (1976), and Chojnacky et al. (2004). Mass per unit area for size classes was estimated by multiplying the volume per unit area for each size class by the specific density (Duvall and Grigal, 1999) of wood for that size class.

2.1.3. Analytical methods

Analysis of isotope tracer mercury absorbed within the gold traps took place at the University of Toronto Scarborough using a gold trap amalgamator and thermal desorber with detection via a coupled ICP-MS. Gold trap samples were thermally desorbed on a stream of Hg-free argon and the liberated Hg vapor was collected onto a secondary pure gold trap. The thermally desorbed contents of the second gold trap were introduced into the torch of the ICP-MS, which allowed for the separation of specific Hg isotopes. The ICP-MS detector was optimized to detect ^{202}Hg (the isotope with highest natural abundance) as well as ^{200}Hg and ^{204}Hg (the isotopes that were enriched in the two Hg tracers applied to the experimental plots). The gaseous absorption on gold traps allowed for removal of possible isobaric interferences from ^{204}Pb. Calibration of the hyphenated detection system was achieved with 5-point quantitative manual injections of gaseous Hg obtained from a Tekran 2505 calibration unit ($r^2 > 0.99$). Analytical stability was monitored by manual injection of known quantities of gaseous Hg samples every 10 samples. Stability was good (measured injection recovery = 95 ± 16%) and where recoveries fell >10% from expected values, the ICP-MS was re-calibrated before continuing with analysis. Gold trap desorption efficiency was verified periodically throughout the sampling season (to ensure memory effects were not present) with manual injections of gaseous Hg. Gold traps which exhibited >10% variation of desorbed Hg quantity from that which was injected were removed from further use. Using the method described by Hintelmann and Evans (1997), the amount of Hg desorbed from the gold traps directly attributable to each of the applied tracers, as well as ambient Hg concentrations, was calculated.

Prior to acid digestion, soil and leaf litter samples were freeze dried then homogenized by hand with stainless steel scissors and a quartz mortar and pestle. Samples were microwave digested in pure nitric acid according to US EPA Method 3051A (U.S. Environmental Protection Agency, 2007). The digestate was diluted with de-ionized water and oxidized with 1% (v/v) BrCl prior to analysis. Samples were analyzed using a Tekran 2600 automated mercury system coupled to an ICP-MS for Hg isotope detection (Hintelmann et al., 1995).

2.1.4. Data handling and statistical methods

Gaseous Hg emission measurements (both automated and gold trap measurements) were computed from the measured inlet and outlet concentrations of air sampled from the dynamic flux chambers using the method provided by Carpi and Lindberg (1997). Quality control of

the automated gaseous Hg emissions measurements (herein referred to as TGM flux measurements) was based on analysis of the inter-cartridge concentration difference of gaseous Hg emissions measured using the Tekran 2537A via the method described by Eckley et al. (2011). Chamber blanks for automated gaseous Hg emissions measurements were -0.07 ± 1.2 ng m^{-2} h^{-1} (n = 131). Quality control of the tracer Hg flux measurements made by gold trap was accomplished by determining the practical detection limit achieved during analysis, taking into consideration travel and chamber blanks as well as the analytical variability. Chamber blanks for excess ^{200}Hg and ^{204}Hg were -0.09 ± 0.12 ng m^{-2} h^{-1} and 0.00 ± 0.07 ng m^{-2} h^{-1}, respectively (n = 8). Gold trap measurements were excluded in circumstances where concentrations were below the detection limit. In 2012 no measurements of the ^{200}Hg tracer (applied the year preceding forest harvesting) were above the detection limit and several ^{204}Hg (applied in May following the forest harvesting) measurements were below detection limit and thus were not included in this analysis. Chamber blanks were not subtracted from measured values (as per Kuiken et al., 2008a and others).

Given the temporal limitations of the gold trap measurements (two ~1 hour emission measurements per day) a common variable of daily flux (ng m^{-2} d^{-1}) was calculated for both the TGM measurements and the tracer Hg measurements at each site. Calculation of daily TGM emissions as measured by the Tekran 2537A was achieved by integrating the area under the diel curve of all valid measurements at each site. Due to variability in the total measurement period at each site (most measurements were not exactly 24 h in length) the value of total TGM emissions per measurement period was then weighted to a daily flux. More complex calculations were required to estimate daily fluxes for tracer Hg measurements. The method used was derived from Engle et al. (2001) who utilized two emission measurements, representing maximum and minimum emission conditions, measured at solar noon and at night, to approximate a daily flux by extrapolation assuming a Gaussian diel pattern of Hg emissions. We modified the technique wherein a four factor Gaussian curve (accounting for: peak width, peak height, peak placement, and curve baseline) was fitted to the TGM emission data to better account for the narrower diel peak in Hg emissions in northern Minnesota compared to the desert environment studied by Engle et al. (2001). Each curve, which more closely approximated the actual flux patterns observed at any given time, was then used to estimate and scale the tracer Hg measurements from the matching time period appropriately. The calculation of daily fluxes, via the Gaussian calculation, modified from Engle et al. (2001), was performed as follows:

$$F_{\mathrm{Daily}} = \int_{t=0}^{t=1} F_{\mathrm{b}} + \left(F_{\mathrm{p}} - F_{\mathrm{b}}\right) e^{\left(-0.5\left(\frac{t-t_{\mathrm{peak}}}{b}\right)^2\right)}.$$

Two key parameters were required from the Gaussian fit of the TGM data, t_{peak} (time of peak TGM emission) and b (the observed TGM emission peak width which was approximately equivalent to the period of daylight). Tracer Hg flux measurements at solar noon (peak flux, F_{p}) and at night (background flux, F_{b}) were utilized to integrate the diel curve (from t = 0: 00:00 to t = 1: 24:00) and thereby estimate the diel flux from each of the sites. Although tracer Hg fluxes were small compared to ambient fluxes, we subtracted mean tracer fluxes from ambient daily fluxes when expressing ambient TGM fluxes.

Statistical analyses were performed using SAS 9.3. Datasets were checked for normality using the Shapiro–Wilk test (Shapiro and Wilk, 1965) before statistical comparisons. When data were normally distributed, which included the TGM flux measurements, parametric statistics were utilized. Log transformations were applied to any datasets not normally distributed, such as the ^{204}Hg fluxes, with parametric statistics applied to the transformed data. Two-way ANOVA tests with Bonferonni post-hoc comparisons (Dunn, 1961) were utilized to highlight differences in observed fluxes among treatments and seasons as well as the overall interaction due to the combined effect of seasonal and treatment variation. One-way ANOVA tests with Tukey post-hoc analyses (Kramer, 1956) were utilized to further investigate differences among individual sites or seasons, which may not be highlighted in a broader two-way ANOVA. Where data could not be successfully transformed into a normal distribution (several of the ancillary environmental variables) non-parametric statistical tests such as the Spearman rank-order correlation (Spearman, 1904) test were conducted. All statistical tests were performed with $\alpha = 0.05$.

3. Results and discussion

3.1. Forest harvesting treatments/woody debris

The masses of downed woody debris increased after the clearcut + biomass and clearcut treatments with the largest increases occurring on the clearcut plot (Fig. 2). Three fold increases in CWD and FWD were measured after the clearcut treatment, when compared to the unharvested control (Fig. 2). An approximate 100% increase in FWD and ~12% increase in CWD debris was observed on the clearcut + biomass plot after harvesting when compared to the control (Fig. 2). Since the threshold for biomass removal was >2.5 cm in diameter, much of the removed biomass was CWD with the woody debris that was not removed nearly all FWD.

3.2. TGM fluxes

Forest harvesting had a substantial effect on TGM fluxes from forest soils, with the greatest impact observed on the clearcut + biomass harvested plot. Forest harvesting led to wetter soils and substantially more solar radiation reaching the forest floor on both the clearcut and clearcut + biomass plots (Fig. 3A, B). Significant differences in TGM fluxes were identified by forest harvesting type ($p = 0.024$; Fig. 3C). Over the entire period of measurement TGM fluxes were significantly different between the control and the clearcut + biomass plots. Fluxes from the clearcut + biomass plot were not significantly different from

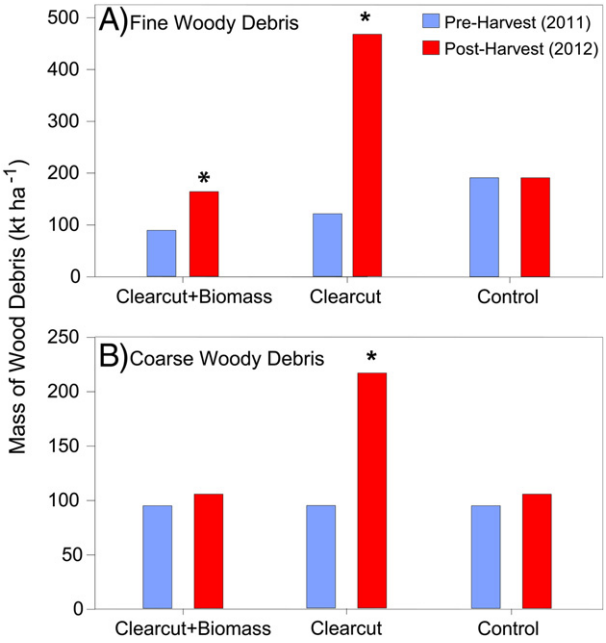

Fig. 2. Fine woody debris (FWD, <7.6 cm diameter) and coarse woody debris (CWD, >7.6 cm diameter) inventory represented as mass per area and grouped by treatment. Inventories were performed prior to harvesting (2011) and following harvesting (2012). Asterisks represent a statistically significant ($\alpha = 0.05$) difference in inventory between pre- and post-harvesting.

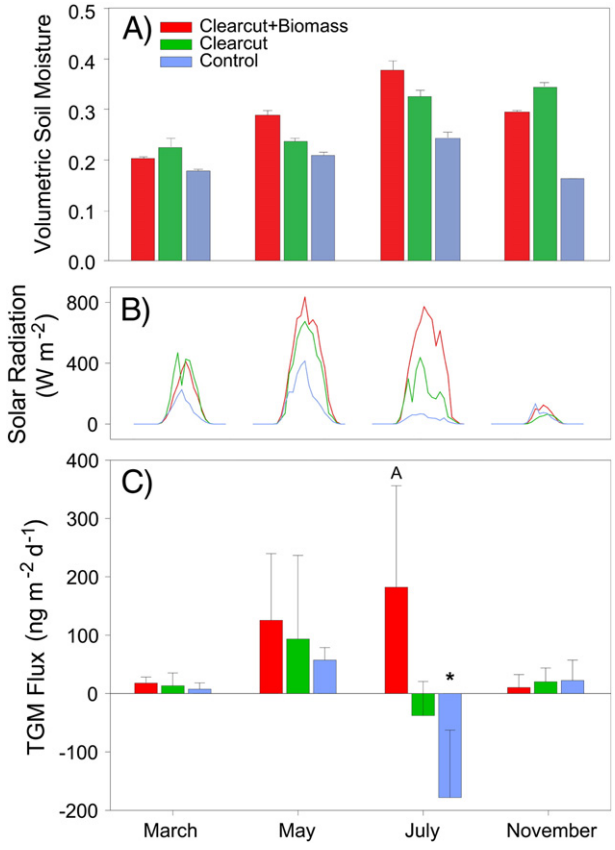

Fig. 3. A) Seven-day mean ± standard deviation of volumetric soil moisture at 1-cm depth on each plot during each period of measurement. B) Average diel solar radiation measured at the forest floor on each plot during each sampling campaign. C) Plot of mean daily TGM fluxes in each plot, grouped by sampling date ($n = 4$ at each site for each season). Error bars represent standard deviations of the mean daily flux. Letter "A" on clearcut + biomass plot in July represents statistically different ($\alpha = 0.05$) mean daily flux as compared to measurements from the other plots during the same season. Asterisk on control plot represents a significant seasonal difference ($\alpha = 0.05$) within the control plot during July compared to the remainder of the year.

the clearcut plot and fluxes from the clearcut and control plots were also not statistically different from one another.

Seasonal differences in TGM emissions between the plots were evident and enhanced by treatment effects. This was particularly evident during the growing season when the control plot was under the shade of a full canopy. The average TGM flux from all three plots in July was significantly different than in May, but was not statistically different than the flux measured in March or November ($p = 0.004$; Fig. 3C). The mean TGM fluxes in March, May and November were statistically indistinguishable from each other. Within seasons, differences in TGM fluxes as a function of treatment were only evident in July, with fluxes from the clearcut + biomass treatment being significantly greater than the fluxes from the clearcut or control plot ($p = 0.033$; Fig. 3C), which both showed average net deposition during this period. July TGM fluxes from the control plot were significantly less than those measured in any other season ($p = 0.014$; Fig. 3C).

The solar radiation flux reaching the forest floor during the growing season (May and July) was highest for the clearcut + biomass treatment, slightly lower for the clearcut treatment and substantially lower for the control (Fig. 3B). Differences in March and November among treatments were not as evident. The removal of forest vegetation clearly increased the flux of incident solar radiation reaching the forest floor (Choi and Holsen, 2008; Kuiken et al., 2008a), particularly when it could be affected by leaf-out in the control plot. Since biomass harvesting removes a larger quantity of vegetation than traditional clearcutting, the soil surface becomes exposed to proportionately more solar radiation. A comparative ratio of measured incident solar radiation, on each of the three plots, to the solar radiation measurements obtained from the nearby and treeless peatland, Bog Lake was calculated. This ratio was then used to better isolate the relative effects of canopy removal on incident radiation levels as a result of forest harvesting. During March and November, when non-harvested trees retained no foliar shading, the mean net radiation received, as a fraction of the radiation measured at Bog Lake was: 1.06 for the clearcut + biomass treatment, 0.77 for the clearcut treatment and 0.60 for the control. During May and July, when non-harvested trees contributed maximal foliar shading and understory vegetation was present, these ratios were different: 1.16 for the clearcut + biomass treatment, 0.96 for the clearcut plot, and most noticeably so, 0.15 for the control. Regeneration of vegetation on the harvested plots increased the shading on these plots through the year resulting in reduced fractions of incident radiation to the soil surface in comparison to Bog Lake in November and as a result the March/November ratio for the clearcut + biomass and clearcut plot were less than that calculated for May/July. In comparison to the control plot, substantial increases in the magnitude of solar radiation reaching the soil surface on the clearcut + biomass and clearcut plots (to levels nearly as strong as from the tree-free Bog Lake) were evident as a result of forest harvesting.

Observed TGM emissions from the soils on the clearcut + biomass and clearcut plots closely mirrored the changes observed in solar radiation magnitude to the soil surface, especially when compared with the control plot; soils with the least vegetative shading (clearcut + biomass) exhibiting the highest magnitude TGM emissions during the growing season. The large quantity of woody debris (CWD and FWD) left on the clearcut plot after harvesting contributed to some shading and likely resulted in the lower Hg emissions observed from this plot. Shading increases, as a result of canopy foliage development on the control plot, resulted in a substantial reduction in daily maximum solar radiation to the forest floor and was associated with substantial TGM deposition. Clearly, with ~85% of the biomass removed from the clearcut + biomass plot, very little of the forest floor was shaded, and the six-fold difference in the magnitude of incident radiation at the soil surface, in comparison to the control plot, likely acted as the strongest factor forcing the increased TGM fluxes observed from this plot.

Within a single season patterns of TGM flux closely mirrored patterns of incident solar radiation, but cross-season observation at times revealed patterns that could not be singularly explained by differences in solar radiation. For example, TGM emissions from the clearcut and clearcut + biomass harvest plots in March were substantially lower than in the control plot in May despite very similar solar radiation inputs. November TGM emissions were comparable to those in March, despite substantially less solar radiation input in November. Soil moisture varied seasonally and may have contributed to some of the differences in flux, however it did not appear to be a strongly controlling factor affecting the overall magnitude of emissions between seasons. The seasonal variation in soil temperatures more similarly fit the observed seasonal TGM flux pattern, however not across treatments during July when we observed much stronger control by solar radiation. The similarity in TGM fluxes between March and November was mirrored in soil temperatures at 5 cm depth (March: 4.7 ± 1.6 ºC; November: 2.8 ± 1.0 ºC), while soil temperatures were significantly greater during May (13 ± 2.0 ºC). Overall, these patterns suggest that soil temperature may have affected TGM fluxes, whether through thermal effects or alterations of microbial activity, but that temperature was not as strong a driver of TGM flux as solar radiation during the growing season when differential shading provided a broad range in solar radiation inputs across our treatments.

Spearman correlations between our observed TGM fluxes and incident solar radiation measurements were significant (Table 1; $p = 0.001$), further supporting our shading changes/photo-reduction theory as most influential in promoting emissions. Similarly strong correlative associations between solar radiation magnitude at the soil surface and the observed Hg emissions (up to $r^2 = 0.8$; Gustin et al.

Table 1
Spearman correlation coefficients between variables measured during 2012. Significant correlations ($\alpha = 0.05$) are in bold.

	Solar radiation	Soil moisture content	THg soil concentration	THg leaf concentration	Air temperature	Soil temperature
Daily average TGM flux	**0.45**	0.17	0.08	−0.04	−0.07	−0.18
Daily average tracer (^{204}Hg) flux	0.22	−0.28	–	–	**−0.58**	–

(2004)) can be found in the literature from soils exposed to direct solar radiation (Carpi and Lindberg, 1997; Kuiken et al., 2008a; Poissant and Casimir, 1998). Substantial increases, by as much as an order of magnitude, in Hg fluxes from deforested soils within the Amazon basin were noted by Almeida et al. (2009) and Magarelli and Fostier (2005). In a more closely related experiment utilizing large mesocosms and aspen poplar saplings, Gustin et al. (2004) noted a substantial increase in fluxes from soils where the saplings had been removed (Gustin et al., 2004). In all of these cases, open canopies allowed enhanced photoreduction to occur at the surface and facilitated higher magnitude Hg fluxes than those measured under a fully shaded canopy where solar radiation to the soil is reduced.

Canopy shading through the growing season limits the magnitude of Hg emissions to less than those observed under canopies with minimal shading, regardless of higher air and soil temperatures experienced during these periods (Denkenberger et al., 2012; Gustin et al., 2004; Gustin and Stamenkovic, 2005; Kuiken et al., 2008a; Sigler and Lee, 2006). We observed a similar pattern in the TGM fluxes from the control plot, and to a lesser degree the clearcut plot, during peak growing season, although net deposition in the clearcut plot was substantially less. Our results mirror recent studies, which have observed Hg fluxes from deciduous forest soils and have highlighted the prevalence of net deposition during daylight hours in the peak growing season. Kuiken et al. (2008a, 2008b) observed substantial deposition, accounting for as much as 50% of the observed Hg fluxes, beneath full canopies across a range of deciduous forests in eastern North America. Similar Hg flux measurements from a boreal forest in Norway also indicated the presence of episodic deposition under a canopy with maximal foliar shading (Kylonnen et al., 2012).

Clearly canopy shaded forest soils, especially those with significant leaf litter layers, are likely subject to complex mechanisms driving fluxes in the absence of strong forcing variables such as large solar radiation inputs, resulting in periodic Hg deposition (Kuiken et al., 2008a). Atmospheric Hg concentrations are a potential driver for variations in soil Hg fluxes (Kuiken et al., 2008a; Kylonnen et al., 2012; Wallschlager et al., 2002). Ambient atmospheric Hg concentrations at ground level (as measured at the intake of the flux chamber) were elevated on every plot in July (overall average: 16.4 ± 10.5 ng m^{-3}), in comparison to the other seasons as well as ambient background concentrations from similar sites (1.56 ± 0.22 ng m^{-3} at the Experimental Lakes Area, ON, Canada; Cheng et al., 2012). We hypothesize that stagnant buildup of Hg in air near the ground surface (Kylonnen et al., 2012) due to low wind speed or a shallower surface boundary layer could be responsible for the episodic presence of high Hg concentrations in ambient air, as has been observed previously by others (Kuiken et al., 2008a). The elevated near surface air concentrations, coupled to lower incident radiation likely crossed the threshold wherein net deposition was favorable (Kuiken et al., 2008a; Wallschlager et al., 2002) in the control, and to a lesser extent, the clearcut plots. A relatively strong, negative Pearson correlation coefficient ($\rho = -0.71$) between the ambient atmospheric Hg concentrations and the observed TGM emissions in July, on the control plot, is further suggestive of a link between the high ambient air Hg concentrations observed near the soil surface and episodes of Hg deposition.

3.3. Tracer fluxes and mass balance estimate

Our observations of the behavior of the ^{204}Hg (applied 2012) and ^{200}Hg (applied 2011) tracers suggest that some of the deposited Hg is very quickly re-emitted following application and that the remaining pool associated with the soil becomes less available for emission over the ensuing months/seasons (Fig. 4). For example, emissions of the ^{204}Hg tracer were elevated (36 ± 29 ng m^{-2} d^{-1}) in May, measured a week after application; however these fluxes declined sharply and significantly by July ($p = 0.002$). The significant negative correlation between tracer Hg flux and air temperature ($\rho = -0.58$, $p = 0.012$; Table 1) also highlights this decline, indicating that even under warmer and sunnier conditions during July, tracer Hg fluxes were substantially lower. By November (6 months after the isotope application) ^{204}Hg fluxes were below detection. The colder temperatures and lower solar radiation in November may have also contributed to the lack of a ^{204}Hg flux being detected (Fig. 3B). However, even during the warmer spring and summer conditions one year following the application of the ^{200}Hg isotope in 2011, the tracer was not detected in flux measurements. Despite the lack of detectable emissions, there remained a substantial pool of tracer Hg measured in the soil/leaf litter during this time (e.g. up to 7.4 μg ^{204}Hg m^{-2} in the control plot; Fig. 5). This surface-bound tracer Hg may not have been available for emission due to shading by fresh leaf litter that was deposited in the fall and/or due to effective sequestration/complexation with the soil or vegetation matrix (Converse et al., 2010; Kylonnen et al., 2012). Overall, it is likely that substantial re-emission of current atmospheric Hg deposition is measurably confined to a period less than a year.

Unlike the increases in TGM fluxes observed from the clearcut + biomass and clearcut treatments, no significant differences in fluxes of tracer Hg were observed with respect to forest treatments ($p = 0.592$; Figs. 3C and 4). Identification of such trends may have been partially obscured by the large variability in the tracer Hg fluxes (standard deviations equivalent to or larger than the tracer flux magnitude); however other factors are also likely at play. Under full canopy conditions in the control plot, emission of the tracer Hg was observed during periods of net TGM deposition. This suggests that even during relatively low-light conditions there was sufficient energy available to promote release of the recently deposited Hg in the upper leaf litter layer (Hintelmann et al., 2002; Sigler and Lee, 2006). Because low levels of solar radiation did not appear to be limiting the release of the tracer Hg, there was not a significant impact on these emissions in response to the increased solar radiation from the harvested plots. We also note that while Hg tracers are the most direct means by which to observe the separate behavior of current Hg deposition and legacy Hg stores in the forest floor, we cannot be entirely sure that our experimental addition of Hg tracers acts exactly as does current Hg deposition. Still, we are confident that Hg tracers applied under low light and rainy conditions, as in this experiment, are likely to partition quickly to favorable organic ligands on the forest floor, such as thiols, as is also likely the case for wet Hg deposition in this region (Xia et al., 1999). Given these caveats, our results suggest that the primary effect of harvest intensity on Hg emissions from soils appears to be the increased activation of additional, non-recent pools of Hg thus accounting for the substantial increase in overall TGM emissions from the clearcut + biomass and clearcut plots. Where substantial canopy shading was present, specifically on the control plot, considerable TGM deposition was observed thereby providing further evidence linking exposure to solar radiation with emissions of non-recent Hg. This may have implications in areas with high soil Hg concentrations where the re-emission of substantial quantities of Hg sequestered in the soil from non-contemporary deposition may occur.

We constructed a rough mass balance for each plot over two periods of measurement in 2012, May through July (59 Days) and July through

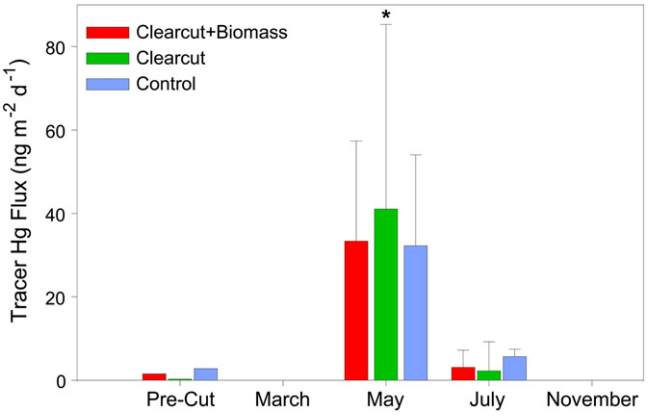

Fig. 4. Plot of mean daily excess ^{200}Hg ("pre-cut" through March) and ^{204}Hg fluxes (May through November) by forestry treatment, grouped by sampling date. Error bars represent standard deviations of the mean daily flux (only single measurements of ^{200}Hg fluxes were made in August 2011). Tracer Hg fluxes across all three plots were significantly greater in May compared to July ($\alpha = 0.05$). No statistically significant differences were determined between treatments in any given season. ^{204}Hg was not applied until May 2012, and fluxes were below detection limit in November 2012. ^{200}Hg fluxes were below detection limit in March 2012.

November (117 days; Fig. 5) to better understand the fate of the ^{204}Hg tracer applied in May 2012, but provide the caveat that there was more than one potential pathway for Hg tracer sequestration or loss that we did not directly measure. In estimating fate of the tracer, we assumed a linear decline in flux rates between seasonal measurements and assumed that the mean tracer load of quadruplicate soil and leaf litter samples was sufficient to account for the spatial variability in tracer sequestration. We note that we did not measure how much of the tracer was sequestered in ground vegetation or downed debris, which presumably could account for most of our inability to close the mass balance at each site, and have illustrated this as the residual to our mass balance in Fig. 5. Hintelmann et al. (2002) quantified the mercury load on all vegetative material within their plots and found it to account for a large proportion (48–66%) of the mercury applied, which is similar to the values we apportion to it as a residual in our mass balance estimate. Hydrological fluxes of applied tracer are also not included in the mass balance, but estimates from our own as yet unpublished work and that of other studies (Hintelmann et al., 2002) suggest that this loss would be no more than 1–2% over these periods of time. Due to experimental constraints, including timing, equipment and sampling related considerations, we must also estimate how much of the tracer

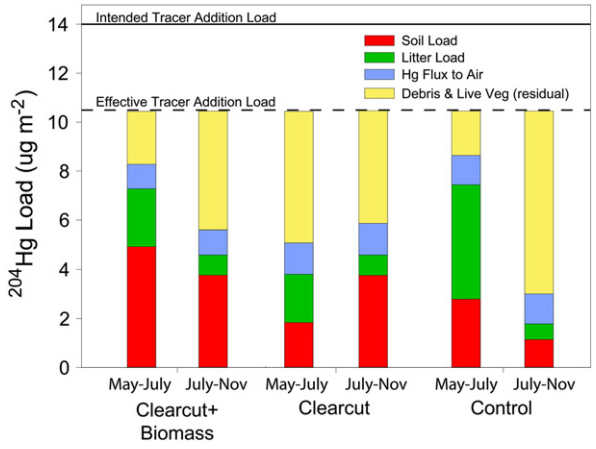

Fig. 5. Mass balance estimate of ^{204}Hg in leaf litter, soil, losses via gaseous emission, and to sequestration in vegetation and downed woody debris (estimated as residual) during the periods May to July and July to November. Dashed line represents the effective tracer Hg addition estimated for the study site in May 2012.

addition was lost by reduction and volatilization of the Hg from the mist produced from the backpack sprayers, previously estimated by Ericksen et al. (2005) to be as much as 25% of the tracer Hg that we measured at the outlet of the sprayer nozzle. We note that we were unable to make direct measurements of the forest litter for tracer Hg concentrations or of fluxes to the atmosphere in the day immediately following the application of the tracer, but rather our first measurements were within 7 days. Given the quantity of tracer Hg lost during application by Ericksen et al. (2005; 25%), we estimate our initial surface loading as likely closer to 10.5 μg m^{-2} (Fig. 5).

Tracer Hg fluxes as a proportion of the total applied tracer over the course of the period of measurement were a modest 8% on average (7.3%, 9.2% and 8.8% for the clearcut + biomass, clearcut and control plots, respectively). Significantly more of the applied ^{204}Hg tracer is being sequestered in surface litter and soil (Fig. 5). Tracer Hg was principally detected in the soil shortly after its application in May (3.1–8.4 μg m^{-2}) with lesser amounts detected within the leaf litter in the clearcut + biomass plot. Reduced leaf litter on the clearcut + biomass plot, due to transport associated with the increased wind velocity at the forest floor (Chen, 1993), was most likely responsible for greater soil exposure and the higher soil tracer Hg load initially on this plot. Enhanced disturbance of the leaf litter on the clearcut + biomass may have also been caused by the additional harvesting equipment traffic needed to complete the treatment; however direct quantification of leaf litter deterioration or transport as a result of this traffic was not performed. Leaf litter loads of ^{204}Hg decreased substantially and soil loads of ^{204}Hg increased, with some variation, in each of the plots between the May to July and July to November periods (Fig. 5). Both the clearcut + biomass and control plots exhibited drops in the ^{204}Hg load in the soil between July and November (Fig. 5). Within days of application, measurements of gaseous emission of the tracer Hg were similar from each plot. Between May and July an equivalent of approximately 1.1 μg ^{204}Hg m^{-2} was lost to the atmosphere. Due to the much lower emissions of the tracer in July and November as compared to May, but longer period of time, an average of 0.5 μg ^{204}Hg m^{-2} to the atmosphere could be estimated from July through November.

Our observations of limited re-emission of deposited Hg are similar to those found in related studies, which have utilized tracer Hg to investigate re-emission and fate. Overall, such results are strongly indicative of the transient nature of recently deposited mercury pools as sources of emitted Hg (Ericksen et al., 2005; Hintelmann et al., 2002). Our observation of 8% re-emission of the applied tracer, through the growing season, agrees well with both Hintelmann et al. (2002) and Ericksen et al. (2005), despite surface characteristics being different among the studies. Both studies reported strong emissions of tracer Hg immediately following application, and on an annualized basis, as well as suggested that overall re-emission of the applied tracer was modest, approximately 8% and 6%, respectively.

Rapid transport of the tracer out of the leaf litter occurred either as losses via emissions or as transport into the upper organic soil horizon, as indicated by our tracer mass balance (Fig. 5). We are able to infer that only a small proportion of recently deposited Hg is available for emission and that the vast majority is sequestered within the soil and leaf litter. Hintelmann et al. (2002) and Ericksen et al. (2005) both noted that Hg volatility with respect to emission is rapidly reduced following deposition over a period of days to weeks as it is sequestered quickly in large proportions into the soil. Reductions in tracer Hg at the soil surface following rainfall events are likely indicative of infiltration of Hg into the upper soil as the primary source of sequestration (Ericksen et al., 2005; Munthe et al., 2001). While we did not make measurements of tracer Hg concentrations in direct relation to individual rainfall events, numerous rainfall events occurred between our May, July and November measurement campaigns. In conjunction with our observation of increased concentrations of tracer Hg in the upper soil with time, we expect that these rainfall events resulted in the downward transport of the tracer. A significant correlation ($\rho = 0.57$; $p = 0.013$), relating the

reduction in leaf litter concentration throughout the year with reduced tracer Hg fluxes, confirms this. Long-term (more than two seasons) data regarding tracer Hg emission from soils are currently not available. However given the current evidence it is expected that once deposited and sequestered, Hg must undergo chemical transformations for some time within the soil before becoming available for emission (Ericksen et al., 2005).

Overall, only 22–62% of the 14 μg $^{204}Hg\ m^{-2}$ of tracer applied to the study site was accounted for across the three compartments measured for Hg tracer (Fig. 5). The clearcut plot consistently had the smallest proportion of the applied tracer Hg apportioned to its various components (36%; Fig. 5). The variability across triplicate measurements on each plot was also large (standard deviation of ±20%), adding to uncertainty in our mass balance, and likely indicates a high degree of spatial heterogeneity in our measurements. Manual addition of the tracer with backpack mounted sprayers is likely a large contributor to the spatial heterogeneity. Variability in vegetation composition, leaf litter cover, the complexity of downed debris, and even soil composition between sites may have also enhanced variability in our results. Additionally, replicate measurements from each site, due to disturbance imparted by sampling of leaf litter and soil, could not be made and therefore we sampled as many as 27 different mid-slope sites on each plot throughout the course of the study.

4. Conclusions

Different forest harvesting practices have differing effects on gaseous mercury flux from forest soils. There are immediate effects due to forest canopy disturbance that increase the magnitude and reverse the TGM flux net direction towards emission. TGM fluxes increase significantly when biomass is harvested following clearcutting. Impacts due to biomass harvesting are strongest during the growing season and if conducted across large geographic areas, such as cutting rotations where large areas are cumulatively cut as several more frequent but smaller harvests, these emissions may be important contributors to the atmospheric Hg load, although significantly more research is necessary to provide representative up-scaling estimates. In terms of more recently deposited Hg (represented by the added enriched stable isotope tracers in this study), substantial proportions are quickly sequestered within the soil, regardless of the degree of disturbance. It is expected that with increasing levels of disturbance the relative contribution of recent deposition to emissions is diminished, as non-recent pools of mercury become readily available for emission. With any degree disturbance to mature forests the overall potential for increased Hg emissions from forest soils is substantial.

Acknowledgments

Funding for this project was provided through a NSERC Discovery grant and Great Lakes Air Deposition Program to CPJM, as well as a University of Toronto Graduate Fellowship to MM. We thank the members of the Mitchell research group for their assistance with all aspects of this experiment, especially the help of Planck Huang for sample analysis. We also wish to thank the staff at the Marcell Experimental Forest Research Station and the cooperation of the USDA Forest Service, without which the bulk of this research would not be possible. In particular we thank Nate Aspelin, Josh Kragthorpe, Reid Peterson, Leigh Kastenson, Paul Watson, Ross Bentson, Mike Palmer, Doris Nelson, Nicole King, Gerrard Graves, Donna Olson, Anne Timm, and Carrie Dorrance of the USFS Northern Research Station and Jeromie Geroatte and Stephen Stalheim of the US Job Corps for their assistance with field work. Finally, we thank Mr. Dwight Streblow for harvesting the plots in 2012. This research does not reflect the official positions and policies of the US EPA. Mention of products/trade names does not constitute recommendation for use by US EPA.

References

Almeida MD, Marins RV, Paraquetti HHM, Bastos WR, Lacerda LD. Mercury degassing from forested and open field soils in Rondonia, Western Amazon, Brazil. Chemosphere 2009; 77:60–6.
Handbook for inventorying downed woody material. Ogden, Utah: US Department of Agriculture, Forest Service, Intermountain Forest and Range Experiment Station; 1974.
Carpi A, Lindberg SE. Sunlight-mediated emission of elemental mercurty from soil amended with municipal sewage sludge. Environ Sci Technol 1997;31:2085–91.
Carpi A, Lindberg SE. Application of a Teflon dynamic flux chamber for quantifying soil mercury flux: tests and results over background soil. Atmos Environ 1998;32: 873–82.
Chen JF. Contrasting microclimates among clearcut, edge, and interior of old-growth Douglas-fir forest. Agr Forest Meteorol 1993;63:219–37.
Cheng I, Zhang L, Blanchard P, Graydon JA, St Louis VL. Source–receptor relationships for speciated atmospheric mercury at the remote Experimental Lakes Area, northwestern Ontario, Canada. Atmos Chem Phys 2012;12:1903–22.
Choi HD, Holsen TM. Gaseous mercury fluxes from the forest floor of the Adirondacks. Environ Pollut 2008;157:592–600.
Chojnacky DC, Mickler RA, Heath LS, Woodall CW. Estimates of down woody materials in eastern US forests. Environ Manage 2004;33:S44–55.
Converse AD, Riscassi AL, Scanlon TM. Seasonal variability in gaseous mercury fluxes measured in a high-elevation meadow. Atmos Environ 2010;44:2176–85.
Denkenberger JS, Driscoll CT, Branfireun BA, Eckley CS, Cohen M, Selvendiran P. A synthesis of rates and controls of elemental mercury evasion in the Great Lakes basin. Environ Pollut 2012;161:291–8.
Dunn OJ. Multiple comparisons among means. J Am Stat Assoc 1961;56:52–64.
Duvall MD, Grigal DF. Effects of timber harvesting on coarse woody debris in red pine forests across the Great Lakes states, USA. Can J Forest Res 1999;29:1926–34.
Eckley CS, Gustin M, Lin CJ, Li X, Miller MB. The influene of dynamic chamber design on operating parameters on calculated surface-to-air mercury fluxes. Atmos Environ 2010;44:194–203.
Eckley CS, Gustin M, Marsik F, Miller MB. Measurement of surface mercury fluxes at active industrial gold mines in Nevada (USA). Sci Total Environ 2011;409:514–22.
Engle MA, Gustin MS, Zhang H. Quanitfying natural source emissions from the Ivanhoe Mining District, north-central Nevada, USA. Atmos Environ 2001;25:3987–97.
Ericksen JA, Gustin MS, Lindberg SE, Olund SD, Krabbenhoft DP. Assessing the potential for re-emission of mercury deposited in precipitation from arid soils using a stable isotope. Environ Sci Technol 2005;39:8001–7.
Graydon JA, St Louis VL, Lindberg SE, Hintelmann H, Krabbenhoft DP. Investigation of mercury exchange between forest canopy vegetation and the atmosphere using a new dynamic chamber. Environ Sci Technol 2006;40:4680–8.
Gustin MS, Engle M, Ericksen J, Lyman S, Stamenkovic J, Xin M. Mercury exchange between the atmosphere and low mercury containing substrates. Appl Geochem 2006;21:1913–23.
Gustin MS, Ericksen JA, Schorran DE, Johnson DW, Lindberg SE, Coleman JS. Application of controlled mesocosms for understanding mercury air–soil–plant exchange. Environ Sci Technol 2004;38:6044–50.
Gustin MS, Biester H, Kim CS. Investigation of light-enhanced emission of mercury from naturally enriched substrates. Atmos Environ 2002;36:3241–54.
Gustin MS, Stamenkovic J. Effect of watering and soil moisture on mercury emission from soils. Biogeochemistry 2005;76:215–32.
Harris RC, Rudd JWM, Amyot M, Babiarz CL, Beaty KG, Blanchfield PJ, et al. Whole ecosystem study shows rapid fish–mercury response to changes in mercury deposition. Proc Natl Acad Sci 2007;104:16586–91.
Hartman JS, Weisberg PJ, Pillai R, Ericksen JA, Kuiken T, Lindberg SE, et al. Application of a rule-based model to estimate mercury exchange for three background biomes in the continental United States. Environ Sci Technol 2009;43:4989–94.
Hintelmann H, Evans RD, Villeneuve JY. Measurement of mercury methylation in sediments by using enriched stable mercury isotopes combined with methylmercury determination by gas chromatography-inductively coupled plasma mass spectrometry. J Anal Atom Spectrom 1995;10:619–24.
Hintelmann H, Evans RD. Application of stable isotopes in environmental tracer studies — measurement of monomethlymercury (CH_3Hg^+) by isotope dilution ICP-MS and dection of species transformation. Fresenius J Anal Chem 1997;358:378–85.
Hintelmann H, Harris R, Heyes A, Hurley JP, Kelly CA, Krabbenhoft DP, et al. Reactivity and mobility of new and old mercury deposition in a boreal forest ecosystem during the first year of the METAALICUS study. Environ Sci Technol 2002;36:5034–40.
Janowiak MK, Webster CR. Promoting ecological sustainability in woody biomass harvesting. J Forest 2010;108:16–23.
Johnson DW, Benesch JA, Gustin MS, Schorran DS, Lindberg S, Coleman J. Experimental evidence against duffusion control of Hg evasion from soils. Sci Total Environ 2003; 304:175–84.
Kim KH, Yoon HO, Jung MC, Oh JM, Brown RJC. A simple approach for measuring emission patterns of vapor phase mercury under temperature-controlled condition from soil. Sci World J 2012:940413.
Kramer CY. Extension of multiple range tests to group means with unequal numbers of replications. Biometrics 1956;12:307–10.
Kuiken T, Gustin M, Zhang H, Lindberg S, Sedinger B. Mercury emission from terrestrial background surfaces in the eastern USA. II: air/surface exchange of mercury within forests from South Carolina to New England. Appl Geochem 2008a;23:356–68.
Kuiken T, Zhang H, Gustin M, Lindberg S. Mercury emission from terrestrial background surfaces in the eastern USA. I: air/surface exchange of mercury within a southeast deciduous forest (Tennessee) over one year. Appl Geochem 2008b;23:345–55.
Kylonnen K, Hakola H, Hellen H, Korhonen M, Verta M. Atmospheric mercury fluxes in a southern boreal forest and wetland. Water Air Soil Pollut 2012;233:1171–82.

Lin CJ, Gustin MS, Singhasuk P, Eckley C, Miller M. Empirical models for estimating mercury flux from soils. Environ Sci Technol 2010;44:8522–8.
Magarelli G, Fostier AH. Influence of deforestation on the mercury air/soil exchange in the Negro river basin, Amazon. Atmos Environ 2005;39:7518–28.
Miller MB, Gustin MS, Eckley CS. Measurement and scaling of air-surface mercury exchange from substrates in the vicinity of two Nevada gold mines. Sci Total Environ 2011;409:3879–86.
Moore C, Carpi A. Mechanisms of the emission of mercury from soil: role of UV radiation. J Geophys Res 2005;110:D24302.
Moore CW, Castro MS. Investigation of factors affecting gaseous mercury concentrations in soils. Sci Total Environ 2012;419:136–43.
Munthe J, Lyven B, Parkman H, Lee Y, Iverfeldt A, Haraldsson C, et al. Mobility and methylation of mercury in forest soils: development of an in-situ isotope tracer technique and initial results. Water Air Soil Pollut Focus 2001;1:385–93.
Poissant L, Casimir A. Water–air and soil–air exchange rate of total gaseous mercury measured at background sites. Atmos Environ 1998;32:883–93.
Schroeder WH, Beauchamp S, Edwards G, Poissant L, Rasumssen P, Tordon R, et al. Gaseous mercury emissions from natural sources in Canadian landscapes. J Geophys Res 2005;110:D18302.
Schroeder WH, Munthe J. Atmospheric mercury — an overview. Atmos Environ 1998;32:809–22.
Sebestyen SD, Dorrance C, Olson DM, Verry ES, Kolka RK, Elling AE, et al. Long-term monitoring sites and trends at the Marcell Experimental Forest. In: Kolka RK, Sebestyen SD, Verry ES, Brooks KN, editors. Peatland biogeochemistry and watershed hydrology at the Marcell Experimental Forest. Boca Raton: CRC Press; 2011. p. 15–71.
Shapiro SS, Wilk MB. An analysis of variance test for normality (complete samples). Biometrika 1965;52:591–611.
Sigler JM, Lee X. Gaseous mercury in background forest soils in the northeastern United States. J Geophys Res 2006;111:G02007.
Song XX, Van Heyst B. Volatilization of mercury from soils in response to simulated precipitation. Atmos Environ 2005;39:7494–505.
Spearman C. The proof and measurement of association between two things. Am J Psychol 1904;15:72–101.
Stamenkovic J, Gustin MS. Evaluation of use of EcoCELL technology for quantifying total gaseous mercury fluxes over background substrates. Atmos Environ 2007;41:3702–12.
van Wagner CE. The line intersect method in forest fuel sampling. Forest Sci 1968;14:20–6.
van Wagner CE. Practical aspects of the line intersect method. Canadian Forestry Service, Ontario, Canada: Petawawa, Ontario; 1982.
van Wagner CE, Wilson AL. Diameter measurement in the line intersect method. Forest Sci 1976;22:230–2.
U.S. Environmental Protection Agency. Method 3051A: microwave assisted acid degestion of sediments, sludges, soils and oils. Washington, DC: Office of Solid Waste; Economic, Methods, and Risk Analysis Division; 2007.
US Forest Service. Phase 3 field guide — down woody materials, version 5.0. Arlington, VA: Forest Inventory & Analysis National Office; 2010.
Wallschlager D, Kock HH, Schroeder WH, Lindberg SE, Ebinghaus R, Wilken RD. Estimating gaseous mercury emissions from contaminated floodplain soils to the atmosphere with simple field measurement techniques. Water Air Soil Pollut 2002;135:39–54.
Xia K, Skyllberg UL, Bleam WF, Bloom PR, Nater EA, Helmke PA. X-ray adsorption spectroscopic evidence for the complexation of Hg(II) by reduced sulfur in soil humic substances. Environ Sci Technol 1999;33:257–61.
Xin M, Gustin MS, Ladwig K, Pflughoeft-Hasset DF. Air-substrate mercury exchange associated with landfill disposal of coal combustion products. J Air Waste Manage Assoc 2006;56:1167–76.
Xin M, Gustin M, Johnson D. Laboratory investigation of the potential for re-emission of atmospherically derived Hg from soils. Environ Sci Technol 2007;41:4946–51.
Zhang H, Lindberg SE, Marsik FJ, Keeler GJ. Mercury air/surface exchange kinetics of background soils of the Tahquamenon river watershed in the Michigan Upper Peninsula. Water Air Soil Pollut 2001;126:151–69.